Oil & Gas Science and Technology – Rev. IFP Energies nouvelles **76**, 22 (2021)

https://doi.org/10.2516/ogst/2020098

Available online at:
ogst.ifpenergiesnouvelles.fr

REGULAR ARTICLE OPEN ACCESS

Influence of five model parameters on the performance of a CO_2 absorber column by a loaded aqueous MEA solution

Ibtissam Hammouche[1,*], Ammar Selatnia[1], and Sonia Yassa[2]

[1] Fossil Energy Valorization Laboratory, Chemical Engineering Department, National Polytechnic School, 10 Avenue HassenBadi, BP 182, El Harrach, Algiers, Algeria
[2] CY Cergy, Paris Université, 33 Boulevard du Port, 95000 Cergy, France

Received: 28 September 2020 / Accepted: 10 December 2020

Abstract. Rigorous packed-bed absorber modeling and simulation are significant for post-combustion CO_2 capture processes design. Hence, a good knowledge and judicious selection of model parameters are essential to ensure reliable predictions. In this paper, the reactive absorption of CO_2 into loaded aqueous monoethanolamine solution was modeled, furthermore, the effects of five different parameters (kinetic model, enhancement factor, enthalpy of absorption, CO_2 diffusivity, and vapor pressure) were investigated. Finally, this study revealed that some model parameters have a large influence on the column performance, contrary to others. In addition, methods and correlations that generally provide more accurate predictions of the empirical data relative to the other cases involved in this research were determined for each model parameter. It was also found that the model deviation was reduced by 18% and 4% for the liquid temperature and liquids CO_2 loading profiles, respectively, while comparing between the worst and the best case.

Nomenclature

a	Interfacial area [m^2/m^3]
$C_{A.I}$	Free CO_2 molar concentration [mol/ m^3]
$C_{p,G}$	Heat capacity in the gas phase [J/(mol K)]
$C_{P,L}$	Heat capacity in the liquid phase [J/(mol K)]
$C_{p.i}^{(g)}$	Heat capacity of species i in the gas phase [J/(mol K)]
$D_{A,G}$	Gas phase CO_2 diffusivity [m^2/s]
$D_{j,\ L}$	Species j diffusivity in the liquid phase [m^2/s]
D_j°	Species j diffusivity in water [m^2/s]
d_h	Hydraulic diameter [m]
E	Enhancement factor
G_B	Flow rate of carrier gas B [mol/(s m^2)]
He	Henry's constant
h_G	Convective heat transfer coefficient [J/(s K m^2)]
k_2	Kinetic constant [m^3/(kmol s)]
$k_{G.i}$	Component i mass-transfer coefficient in the gas side [kmol/(kPa m^2 s)]
$k_{L.A}^0$	Mass transfer coefficient in the liquid phase [m/s]
L	Liquid flow rate [mol/(s m^2)]
P	Gas-phase total pressure [Pa]
P_S^{sat}	Water vapor pressure [Pa]
T_0	Standard temperature [298.15 K]
T_G	Temperature in the gas side [K]
T_L	Temperature in the liquid bulk [K]
x_s	Mole fraction of water in the liquid phase
y_i	The bulk gas side mole fraction of species i
$y_{i.I}$	Species i mole fraction at the gas side interface
z	Column height [m]

Greek letters

α_{CO_2}	CO_2 loading [mol CO_2/mol MEA]
$\Delta H_{rx}^{(abs)}$	Enthalpy of absorption [kJ/mol of CO_2]
ΔHvap,S	Heat of vaporization of water [J/mol]
ω	Acentric factor
γ_S	Activity coefficient of water in the liquid phase

Subscripts

A	Carbon dioxide
ARD%	Average relative deviation percentage
B	Carrier gas
MEA	Monoethanolamine
R	MEA
S	Water vapor

* Corresponding author: ibtissam.hammouche@g.enp.edu.dz

1. Introduction

Significant efforts have been made to reduce greenhouse gas emissions and mitigate the global warming IPCC (2007). In this area, particular attention has been given to carbon dioxide removal using the post-combustion process on the basis of the absorption-desorption with chemical solvents.

In recent years, remarkable progress has been made in this area of research. New solvents that increase the CO_2 absorption and desorption of CO_2 have been developed such as the nanoparticle additives and biphasic solvents (Liu *et al.*, 2019; Mehassouel *et al.*, 2018; Wang *et al.*, 2016). Despite that, aqueous solution of monoethanolamine is undoubtedly still the most extensive, mature, appropriate, and well-documented chemical solvent for the CO_2 capture in post-combustion processes (Akinola *et al.*, 2019; Ali Saleh Bairq *et al.*, 2019; Gheni *et al.*, 2018; Mohammadpour *et al.*, 2019; Wang *et al.*, 2019).

Reliable dimensioning, scaling, and monitoring post-combustion processes require the use of an accurate packed bed absorber modeling and simulation (Llano-Restrepo and Araujo-Lopez, 2015). Therefore, a good knowledge and judicious selection of model parameters are essential to ensure rigorous predictions. In this context, several studies on diverse process parameters have been published in literature (Abu-Zahra *et al.*, 2007; Afkhamipour and Mofarahi, 2013, 2014; Khan *et al.*, 2011; Kvamsdal and Rochelle, 2008; Kvamsdal and Hillestad, 2012; Mofarahi *et al.*, 2008; Wu *et al.*, 2010).

Abu-Zahra *et al.* (2007) investigated absorber inlet temperature, lean amine loading, concentration, and stripper pressure sensitivities. Furthermore, the process that recovers carbon dioxide from flue gas was studied by Mofarahi *et al.* (2008) where the effect of both operating conditions and design parameters on the absorber and stripper columns was presented. In addition, a statistical analysis and a combination between the sensitivity analysis and the neural networks modeling were carried out by Wu *et al.* (2010) to investigate the interactions between similar main process parameters. However, the studies on the selection of rate-based model parameter correlations in packed columns are scarce. Khan *et al.* (2011) applied the rate-based model to perform a sensitivity analysis using different mass transfer coefficients in a packed column. Furthermore, in the aim of determining the temperature bulge position and magnitude, Kvamsdal and Rochelle (2008) carried out a comparative analysis between diverse methods that compute mass transfer coefficient, liquid heat capacity, and liquid density. Moreover, Kvamsdal and Hillestad (2012) focused on the selection of the rate-based model parameter correlations for prediction of physical properties and kinetics, they investigated also their effects on mass and energy balances. Afkhamipour and Mofarahi (2013, 2014) performed a rate-based model sensitivity analysis, once by varying different mass transfer correlations, and another time by combining these correlations with different kinetic models.

In the current paper, the reactive absorption of CO_2 with loaded aqueous monoethanolamine solution in a packed-bed absorber was modeled and simulated, in addition, the effects of five different parameters (kinetic model, enhancement factor, enthalpy of absorption, CO_2 diffusivity in aqueous solution of MEA, and vapor pressure) on the column performance were investigated by performing a parametric study based on step-by-step approach.

2 Rate-based model

For modeling the CO_2 absorption in a packed column, three forms of the rate-based model were developed: the Continuous Differential Contactor (CDC) model, the Continuous Film Reaction (CFR) model, and Non-Equilibrium Stage (NEqS) model. In this study, the last version of the CDC model was applied, indicating that this model was first proposed by Pandya (1983) based on the differential-change approach suggested by Treybal (1969) which was largely employed by many authors, and since it presents some inconsistent simplifications or assumptions, Llano-Restrepo and Araujo-Lopez (2015) revised the model using the finite difference approach and introduced a new improved version as shown below:

CO_2 and water vapor balances for the gas phase:

$$\frac{\mathrm{d}Y_{\mathrm{A}}}{\mathrm{d}z} = \frac{-k_{\mathrm{G.A}}\, aP(y_{\mathrm{A}} - y_{\mathrm{A.I}})}{G_{\mathrm{B}}}, \tag{1}$$

$$\frac{\mathrm{d}Y_{\mathrm{S}}}{\mathrm{d}z} = \frac{-k_{\mathrm{G.S}}\, aP(y_{\mathrm{S}} - y_{\mathrm{S.I}})}{G_{\mathrm{B}}}. \tag{2}$$

The mole fractions of CO_2 and water vapor $y_{\mathrm{A.I}}$ and $y_{\mathrm{S.I}}$, respectively, at the interface are given below:

$$y_{\mathrm{A.I}}P = \frac{y_{\mathrm{A}}P + \left(\frac{Ek^0_{\mathrm{L.A}}}{k_{\mathrm{G.A}}}\right) C_{\mathrm{A}}}{1 + \frac{1}{\mathrm{He}}\left(\frac{Ek^0_{\mathrm{L.A}}}{k_{\mathrm{G.A}}}\right)}, \tag{3}$$

$$y_{\mathrm{S.I}} = x_{\mathrm{S}}\, \gamma_{\mathrm{S}}\, P^{\mathrm{sat}}_{\mathrm{S}}/P. \tag{4}$$

Noting that, the model considers the liquid phase as an ideal solution. Thus $\gamma_{\mathrm{S}} = 1$ and Raoult's law $y_{\mathrm{S.I}} = x_{\mathrm{S}}\, P^{\mathrm{sat}}_{\mathrm{S}}/P$ is valid.

- A total mole balance for both liquid and gas phases:

$$\frac{\mathrm{d}L}{\mathrm{d}z} = G_{\mathrm{B}}\left(\frac{\mathrm{d}Y_{\mathrm{A}}}{\mathrm{d}z} + \frac{\mathrm{d}Y_{\mathrm{S}}}{\mathrm{d}z}\right). \tag{5}$$

- Temperature gradients for the gas and liquid phases:

$$\frac{\mathrm{d}T_{\mathrm{G}}}{\mathrm{d}z} = \frac{-h_{\mathrm{G}}(T_{\mathrm{G}} - T_{\mathrm{L}})\, a}{G_{\mathrm{B}}\left(C^{(\mathrm{g})}_{\mathrm{p.B}} + Y_{\mathrm{A}} C^{(\mathrm{g})}_{\mathrm{p.A}} + Y_{\mathrm{S}} C^{(\mathrm{g})}_{\mathrm{p.S}}\right)}, \tag{6}$$

$$\frac{\mathrm{d}T_L}{\mathrm{d}z} = \frac{G_\mathrm{B}}{LC_\mathrm{P,L}}\left\{\left(C^{(\mathrm{g})}_{\mathrm{p.B}} + Y_\mathrm{A}C^{(\mathrm{g})}_{\mathrm{p.A}} + Y_\mathrm{S}C^{(\mathrm{g})}_{\mathrm{p.S}}\right)\frac{\mathrm{d}T_\mathrm{G}}{\mathrm{d}z}\right.$$
$$+\left[\int_{T_0}^{T_\mathrm{G}} C^{(g)}_{\mathrm{p.A}}\,\mathrm{d}T - \Delta H^{(\mathrm{abs})}_{rx}(T_0) - \int_{T_0}^{T_\mathrm{L}} C_\mathrm{P,L}\mathrm{d}T\right]\frac{\mathrm{d}Y_\mathrm{A}}{\mathrm{d}z}$$
$$\left.+\left[\int_{T_0}^{T_\mathrm{G}} C^{(\mathrm{g})}_{\mathrm{p.S}}\,\mathrm{d}T - \Delta H_{\mathrm{vap,S}}(T_0) - \int_{T_0}^{T_\mathrm{L}} C_\mathrm{P,L}\mathrm{d}T\right]\frac{\mathrm{d}Y_\mathrm{S}}{\mathrm{d}z}\right\}. \quad (7)$$

Indicating that the energy balance neglects heat losses through the wall of the absorber column (an adiabatic column is assumed).

For the resolution of these differential equations a computer program was coded in Matlab software.

The correlations used for estimating the different physicochemical and transport properties are listed in Table A1.

3 Kinetic model

A large number of experimental and theoretical studies have been recorded in literature on the kinetics of the reaction between CO_2 and an uncharged aqueous MEA since 1950s (Blauwhoff *et al.*, 1983; Danckwerts and Sharma, 1966; Faramarzi, 2010; Freguia and Rochelle, 2003; Hikita *et al.*, 1977, 1979; Horng and Li, 2002; Jamal *et al.*, 2006; Kucka *et al.*, 2002, 2003; Kvamsdal *et al.*, 2009; Luo *et al.*, 2012; Pinsent *et al.*, 1956; Plaza, 2011; Versteeg *et al.*, 1996; Ying and Eimer, 2013). However, only few researchers have studied kinetics of CO_2 absorption into partially carbonated MEA solutions (Aboudheir *et al.*, 2003; Dang and Rochelle, 2003; Dugas and Rochelle, 2011; Littel *et al.*, 1992; Luo *et al.*, 2015; Puxty *et al.*, 2010). Among these research works, only two termolecular kinetic models of carbon dioxide reacting with loaded aqueous MEA solution have been found (Aboudheir *et al.*, 2003; Luo *et al.*, 2015), Table A2 includes both models, the mechanism that they are based on and their validity ranges.

4 Enhancement factor

Since the last century, many researchers have studied the enhancement factor used to compute the mass transfer rates from gases to liquids (Brian *et al.*, 1961; Cussler, 2009; DeCoursey, 1982; DeCoursey and Thring, 1989; Gaspar and Fosbøl, 2015; Gilliland *et al.*, 1958; Hatta, 1928; Hikita *et al.*, 1982; Hogendoorn *et al.*, 1997; Last and Stichlmair, 2002; Van Krevelen and Hoftijzer, 1948; Van Swaaij and Versteeg, 1992; Van Wijngaarden *et al.*, 1986; Versteeg *et al.*, 1989; Wellek *et al.*, 1978; Yeramian *et al.*, 1970). Consequently, a great variety of models have been developed (Brian *et al.*, 1961; Cussler, 2009; Gaspar and Fosbøl, 2015; Last and Stichlmair, 2002; Van Krevelen and Hoftijzer, 1948; Wellek *et al.*, 1978; Yeramian *et al.*, 1970). A list of expressions allowing the calculation of enhancement factor is provided in Table A3.

5 Heat of absorption

Although MEA is believed to be the most commonly used solvent for the CO_2 removal, only limited data on the direct measurements of the heat of absorption of the reaction between CO_2 and aqueous solutions of MEA have been published (Arcis *et al.*, 2011; Carson *et al.*, 2000; Kim, 2009; Kim and Svendsen, 2007; Mathonat *et al.*, 1998).

Few researchers, in their works, used fixed values for the enthalpy of absorption prediction (Kohl and Nielsen, 1997; Kvamsdal and Rochelle, 2008; Pandya, 1983), however, others have developed new correlations to calculate the enthalpy of absorption on the basis of existing empirical data available in literature (Kim, 2009, Llano-Restrepo and Araujo-Lopez, 2015). All these correlations and fixed values for the heat of absorption estimation are summarized in Table A4.

6 Vapor pressure

Over the years, various temperature dependent equations for water vapor pressure estimation have been developed. In this study, we will consider the ones that are most commonly used in literature (Ambrose and Walton, 1989, Antoine, 1888, Riedel, 1954). These correlations are written in Table A5.

7 CO_2 diffusivity in aqueous solutions of MEA

Because of the reaction occurring between CO_2 and the amine solutions, the CO_2 diffusivity in the MEA solution cannot be determined directly. Therefore, Clarke (1964) proposed the N_2O analogy method which has been then adopted by many researchers. This approach can be expressed as follows:

$$D_{\mathrm{CO_2,L}} = D_{\mathrm{N_2O,L}}\left(\frac{D^{\circ}_{\mathrm{CO_2}}}{D^{\circ}_{\mathrm{N_2O}}}\right). \quad (8)$$

Various measurements have been reported in literature on the N_2O diffusivity in aqueous solutions of MEA on a broad range of MEA concentration and temperature (Clarke, 1964; Cullen and Davidson, 1957; Sada *et al.*, 1978; Li and Lai, 1995; Ko *et al.*, 2001; Ying and Eimer, 2012). Based on these experimental data, different correlations have been developed which are listed in Table A6.

8 Parametric study

The effects of changing the empirical correlations or fixed values on the column performance (liquid temperature and liquid CO_2 loading profiles) were investigated for each model parameter following step-by-step approach, that

Table 1. Summary of the model parameter correlations used in each cases.

	Kinetic model	Enhancement factor	Enthalpy of absorption	Vapor pressure	CO_2 diffusivity	Number of cases
1. Kinetic model	Variable	Fixed	Fixed	Fixed	Fixed	2 cases
	(a) Luo *et al.* (2015) (b) Aboudheir *et al.* (2003)	Gaspar and Fosbøl (2015)	Llano-Restrepo and Araujo-Lopez (2015) based on Arcis *et al.* (2011) data	Antoine (1888)	Ying and Eimer (2012)	
2. Enhancement factor	Fixed	Variable	Fixed	Fixed	Fixed	8 cases
	Luo *et al.* (2015)	(a) Van Krevelen and Hoftijzer (1948) (b) Brian *et al.* (1961) (c) Yeramian *et al.* (1970) based on penetration theory (d) Yeramian *et al.* (1970) based on surface renewal theory (e) Wellek *et al.* (1978) (f) Last and Stichlmair (2002) (g) Cussler (2009) (h) Gaspar and Fosbøl (2015)	Llano-Restrepo and Araujo-Lopez (2015) based on Arcis *et al.* (2011) data	Antoine (1888)	Ying and Eimer (2012)	
3. Enthalpy of absorption	Fixed	Fixed	Variable	Fixed	Fixed	5 cases
	Luo *et al.* (2015)	Van Krevelen and Hoftijzer (1948)	(a) Kohl and Nielsen (1997) (b) Pandya (1983) (c) Kim (2009) (d) Llano-Restrepo and Araujo-Lopez (2015) based on Kim and Svendsen (2007) data (e) Llano-Restrepo and Araujo-Lopez (2015) based on Arcis *et al.* (2011) data	Antoine (1888)	Ying and Eimer (2012)	
4. Vapor pressure	Fixed	Fixed	Fixed	Variable	Fixed	3 cases
	Luo *et al.* (2015)	Van Krevelen and Hoftijzer (1948)	Llano-Restrepo and Araujo-Lopez (2015) based on Arcis *et al.* (2011) data	(a) Antoine (1888) (b) Riedel (1954) (c) Ambrose and Walton (1989)	Ying and Eimer (2012)	
5. CO_2 diffusivity	Fixed	Fixed	Fixed	Fixed	Variable	3 cases
	Luo *et al.* (2015)	Van Krevelen and Hoftijzer (1948)	Llano-Restrepo and Araujo-Lopez (2015) based on Arcis *et al.* (2011) data	Antoine (1888)	(a) Ko *et al.* (2001) (b) Jamal (2002) (c) Ying and Eimer (2012)	

Table 2. Simulation results for runs (R 3, 8, 13–15, 18, 21–23) of Sonderby *et al.* (2013).

1. Kinetic model		Run 3	Run 8	Run 13	Run 14	Run 15	Run 18	Run 21	Run 22	Run 23
ARD% for the liquid CO_2 loading profile	Case 1-a	3.719	3.373	5.074	5.146	5.188	2.101	2.099	1.552	1.804
	Case 1-b	3.920	4.874	6.291	5.444	6.391	6.556	2.626	2.668	3.568
ARD% for the liquid temperature profile	Case 1-a	2.015	4.278	2.686	2.738	1.823	5.091	2.532	2.530	2.593
	Case 1-b	3.789	6.580	2.910	3.703	2.781	6.442	3.229	4.088	3.643
2. Enhancement factor										
ARD% for the liquid CO_2 loading profile	Case 2-a	3.709	3.359	5.055	5.144	5.174	2.055	2.095	1.550	1.762
	Case 2-b	3.764	3.412	5.111	5.154	5.220	2.213	2.102	1.559	1.833
	Case 2-c	3.736	3.459	5.135	5.170	5.256	2.334	2.101	1.565	1.867
	Case 2-d	3.735	3.461	5.155	5.171	5.258	2.340	2.100	1.565	1.870
	Case 2-e	3.728	3.467	5.152	5.166	5.260	2.350	2.100	1.563	1.867
	Case 2-f	3.733	3.491	5.189	5.191	5.285	2.417	2.100	1.571	1.891
	Case 2-g	3.800	3.595	5.284	5.232	5.361	2.688	2.103	1.600	1.961
	Case 2-h	3.719	3.373	5.074	5.146	5.188	2.101	2.099	1.552	1.804
ARD% for the liquid temperature profile	Case 2-a	2.008	4.260	2.664	2.734	1.814	5.078	2.522	2.521	2.583
	Case 2-b	2.038	4.330	2.744	2.743	1.844	5.125	2.554	2.550	2.610
	Case 2-c	2.061	4.385	2.727	2.749	1.867	5.160	2.579	2.573	2.630
	Case 2-d	2.063	4.387	2.726	2.750	1.868	5.162	2.581	2.574	2.632
	Case 2-e	2.068	4.396	2.716	2.749	1.869	5.164	2.578	2.569	2.625
	Case 2-f	2.073	4.418	2.720	2.756	1.885	5.183	2.603	2.594	2.650
	Case 2-g	2.127	4.540	2.762	2.783	1.934	5.263	2.654	2.642	2.695
	Case 2-h	2.015	4.278	2.686	2.738	1.823	5.091	2.532	2.530	2.593
3. Enthalpy of absorption										
ARD% for the liquid CO2 loading profile	Case 3-a	3.858	3.456	5.153	5.486	5.188	2.286	2.099	1.587	1.767
	Case 3-b	4.394	3.462	5.231	5.565	5.256	2.655	2.158	1.605	1.772
	Case 3-c	4.406	3.464	5.235	5.593	5.259	2.648	2.159	1.606	1.773
	Case 3-d	4.439	3.469	5.244	5.615	5.262	2.666	2.160	1.608	1.782
	Case 3-e	3.709	3.359	5.055	5.144	5.174	2.055	2.095	1.550	1.762
ARD% for the liquid temperature profile	Case 3-a	7.478	6.220	4.871	4.979	4.131	5.190	5.573	5.746	5.239
	Case 3-b	8.961	6.425	9.382	8.889	6.565	5.703	7.793	5.881	5.416
	Case 3-c	9.151	6.603	9.543	9.018	6.763	5.805	7.925	5.944	5.415
	Case 3-d	9.600	7.006	9.916	9.384	6.968	6.091	8.114	6.118	5.623
	Case 3-e	2.008	4.260	2.664	2.734	1.814	5.078	2.522	2.521	2.583
4. Vapor pressure										
ARD% for the liquid CO_2 loading profile	Case 4-a	3.709	3.359	5.055	5.144	5.174	2.055	2.095	1.550	1.762
	Case 4-b	9.361	6.438	7.141	5.794	5.201	3.237	3.839	2.813	3.567
	Case 4-c	3.888	4.825	5.984	5.492	5.199	3.074	2.370	2.003	3.146
ARD% for the liquid temperature profile	Case 4-a	2.008	4.260	2.664	2.734	1.814	5.078	2.522	2.521	2.583
	Case 4-b	15.078	11.868	17.137	17.035	9.689	12.278	18.383	17.308	18.346
	Case 4-c	7.634	9.843	5.712	6.536	4.125	8.212	5.423	6.963	6.908
5. CO_2 diffusivity										
ARD% for the liquid CO_2 loading profile	Case 5-a	3.732	3.516	5.229	5.221	5.252	2.421	2.098	1.591	1.964
	Case 5-b	3.828	5.150	6.107	5.378	6.191	5.961	2.554	2.578	2.884
	Case 5-c	3.709	3.359	5.055	5.144	5.174	2.055	2.095	1.550	1.762
ARD% for the liquid temperature profile	Case 5-a	2.085	4.438	2.739	2.765	1.861	5.178	2.628	2.621	2.673
	Case 5-b	3.567	6.305	2.928	3.516	2.571	6.254	3.115	3.662	3.521
	Case 5-c	2.008	4.260	2.664	2.734	1.814	5.078	2.522	2.521	2.583

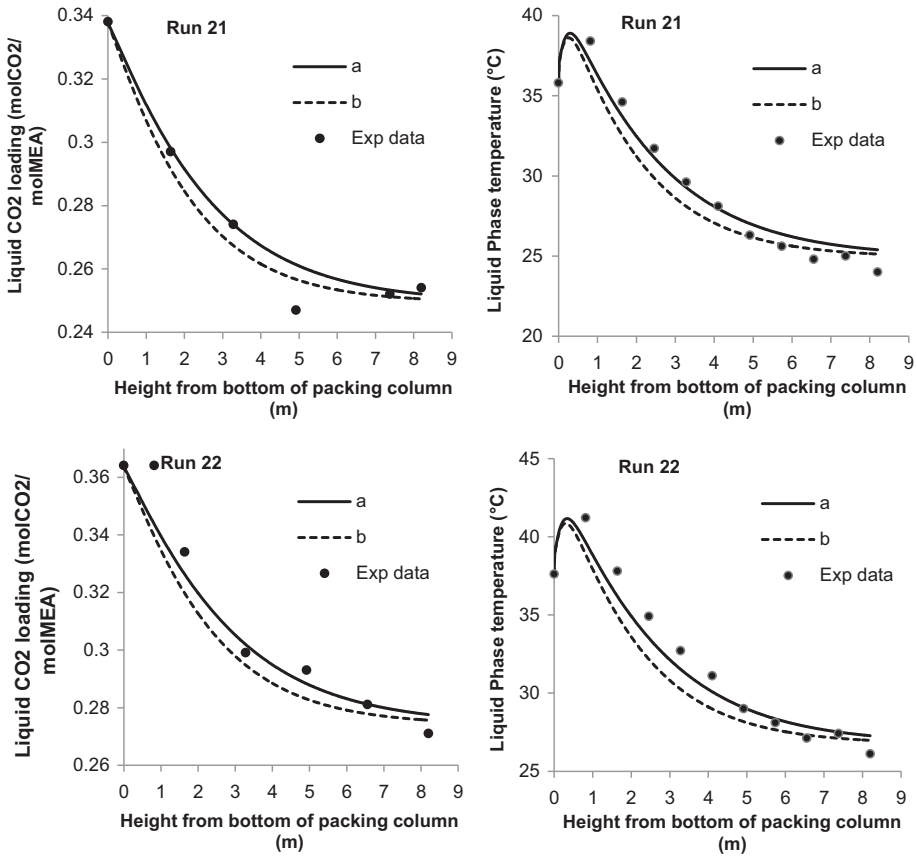

Fig. 1. Simulation results obtained using different kinetic models: (a) Luo *et al.* (2015) and (b) Aboudheir *et al.* (2003).

means, each time the best correlation for the parameter X calculation is determined then used (or fixed) to study the next parameter, and so on. For a better understanding, Table 1 shows the different methods used for model parameters calculation in each case.

In this paper, the average relative deviation percentage ARD% was the criterion used to compare model predictions with experiments, and it was computed by using the following equation:

$$\mathrm{ARD}\% = 100 \times \frac{1}{n}\sum_{1}^{n}\left(\frac{x_i^{\mathrm{cal}} - x_i^{\mathrm{Exp}}}{x_i^{\mathrm{Exp}}}\right). \qquad (9)$$

9 Results and discussion

In this research work, the model simulation was based on the experimental data reported in the literature by Sonderby *et al.* (2013) using a pilot-scale CO_2 absorption column, where 23 experiments were performed, denoted (R1–R23). However, in this study, only 9 runs (R 3, 8, 13–15, 18, 21–23) were taken into account, as shown in Table 2. This selection was founded on two criteria: a low experimental error and a large number of points (measurements) in each run.

All the simulation results, displayed in terms of liquid temperature and liquid CO_2 loading average relative deviation percentages (ARD%s) for all runs (R 3, 8, 13–15, 18, 21–23) and all cases (21 cases), are summarized in Table 2.

In this section, the results presented in Table 2 are discussed in general terms, that means, they will be discussed only in respect of the simulation deviation between the different runs, and then a detailed discussion is given for each parameter separately (in Sects. 9.1–9.5).

The Case 5-c is selected as a base case for this discussion because it represents a combination between the correlations that provide the lowest ARD%. Accordingly, it has been noticed that for the liquid CO_2 loadings, the ARDS% are in the range of 1–6%. A maximum ARD% of ±5% is obtained for runs (R13–15), while the minimum ARD% of ±2% is obtained for runs (R18, 21–23). Furthermore, for the liquid temperature, the ARDS% for the different runs are varying also between 1% and 6%. A maximum ARD% of ±5% is obtained for Run 18, an ARD% of 4.260% is also given by Run 8, while the other runs (R3, 13–15, 21–23) have an ARD% of ±2%. This difference in ARD%s between the different runs might be cause by the experimental errors which are different from a run to another, and it is believed that the reasons of these deviations are: The use of manual instruments instead of digital readouts which

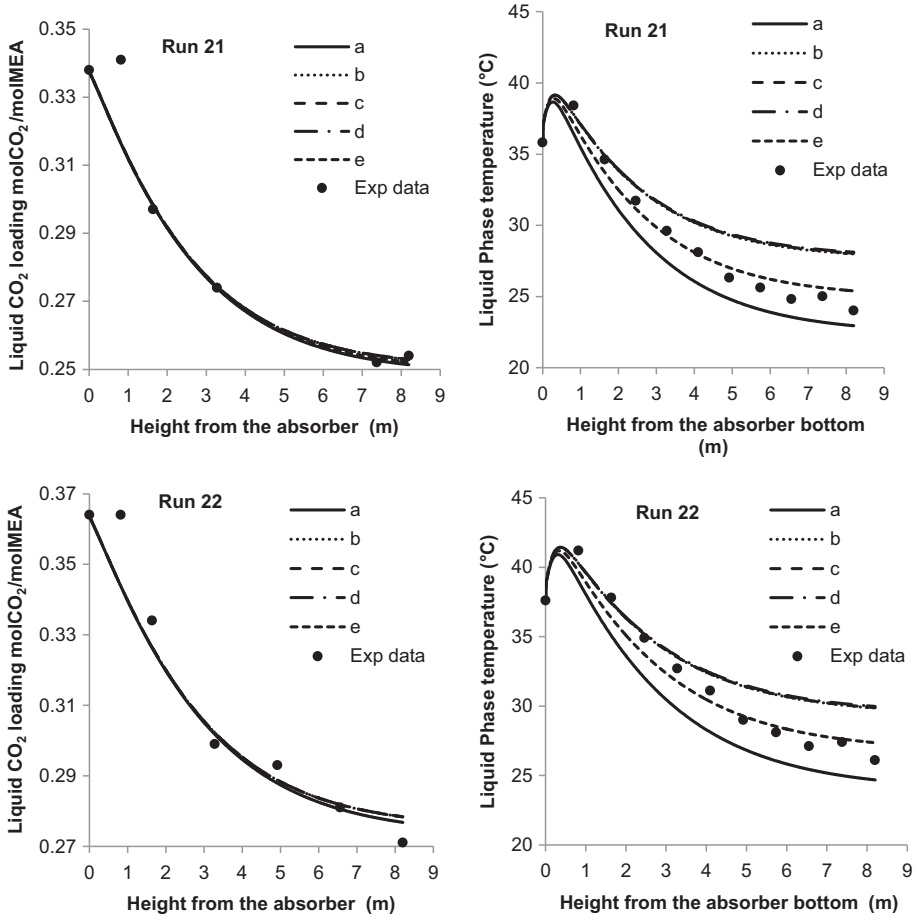

Fig. 2. Simulation results obtained using different approaches of heat of absorption: (a) Kohl and Nielsen (1997), (b) Pandya (1983), (c) Kim (2009), (d) Llano-Restrepo and Araujo-Lopez (2015) based on Kim and Svendsen (2007) data and (e) Llano-Restrepo and Araujo-Lopez (2015) based on Arcis *et al.* (2011) data.

require a calibration prior to each run. Moreover, the difficulty to reach the adiabatic conditions at the laboratory scale which is assumed in the model development. Finally, pressure and heat losses along the column.

9.1 Kinetic model

A sensible selection of kinetic models is important for obtaining accurate predictions. In regards to this area, the liquid-phase temperature and liquid CO_2 loading have been simulated using two different kinetic models (Aboudheir *et al.*, 2003, Luo *et al.*, 2015).

Figure 1 illustrates the simulation results in respect of the empirical values obtained from runs R21 and R22 of Sonderby *et al.* (2013). According to this figure, it has been noticed that the liquid temperature and the liquid CO_2 loading profiles simulated by using the kinetic model suggested by Luo *et al.* (2015) are more accurate than the ones obtained while using the kinetic model of Aboudheir *et al.* (2003). The use of the kinetic model of Aboudheir *et al.* (2003) is somewhat under predicts the liquid temperature and the liquid CO_2 loading. This low accuracy presented by this kinetic model might be affected by the instrumental methods employed to obtain kinetic data, and the empirical correlations of physical properties (CO_2 diffusivity and solubility in aqueous solutions) employed for kinetic model development. Furthermore, it has been also observed that the kinetic models have a large influence on both, liquid CO_2 loading and liquid temperature. And according to the results obtained from Cases 1.a to 1.b for all runs, presented in Table 2, the same conclusions are found.

9.2 Enhancement factor

On the basis of the results presented in Table 2 for the Cases 2.a–2.h, it can be deduced that the effect of the different enhancement factor models on the performance of the columns is not very significant. The ARD%s between the simulation results and pilot-plant measured data are very close for all cases, the difference is in the order of ±0.1% for both liquid temperature and liquid CO_2 loading. The lowest ARD% is obtained by using the model developed by Van Krevelen and Hoftijzer (1948), while the highest ARD% is given from the model suggested by Cussler (2009).

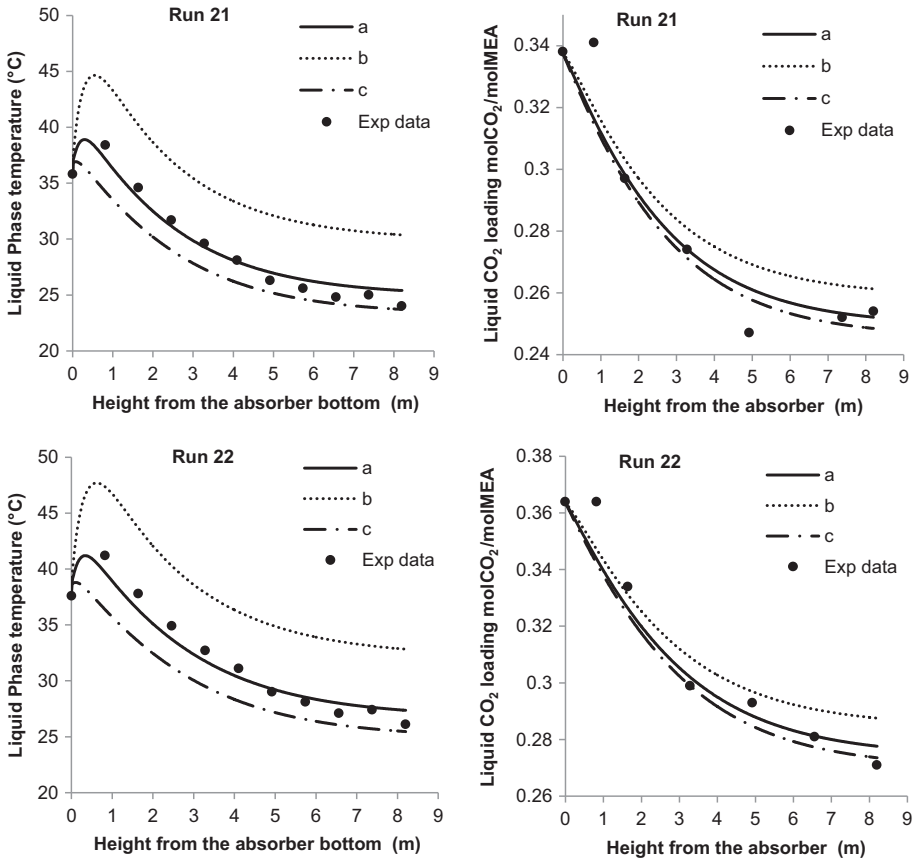

Fig. 3. Simulation results obtained using different cases of vapor pressure correlations: (a) Antoine (1888), (b) Riedel (1954), and (c) Ambrose and Walton (1989).

9.3 Enthalpy of absorption

The simulated liquid temperature and liquid CO_2 loading profiles were compared with measurements taken from runs R21 and R22 of Sonderby *et al.* (2013), as shown in Figure 2, to study the effect of the enthalpy of absorption on the absorber performance.

Accordingly, it has been noticed that the influence of the enthalpy of absorption on the liquid CO_2 loading is very small, the different profiles obtained for R21 and R22 are almost overlapped, there is just a slight difference in the last 3 m of the absorber height, where the lowest ARD% is obtained from the correlation of Llano-Restrepo and Araujo-Lopez (2015) based on Arcis *et al.* (2011). On the other hand, the effect is very high for the liquid temperature profiles. It has been observed that the use of the fixed value of 118.2 kJ/mol, given by Kohl and Nielsen (1997), underpredicts the liquid temperature profile for both runs R21 and R22 with ARD%s of 5.573% and 5.746%, respectively. Furthermore, the liquid temperature profiles obtained by using the fixed value of 84.4 kJ/mol reported by Pandya (1983) and the two correlations developed by Kim (2009) and Llano-Restrepo and Araujo-Lopez (2015) based on Kim and Svendsen (2007) data are closely superposed with ARDs% of 7.793, 7.925, and 8.114%, respectively, for R21, and ARDs% of 5.881, 5.944 and 6.118%, respectively, for R22, they exhibit a good accord with experimental data in the initial 3 m then they overpredict the liquid temperature for the rest of the column. Finally, the correlation suggested by Llano-Restrepo and Araujo-Lopez (2015) based on Arcis *et al.* (2011) data provides the lowest ARD% of 2.522% and 2.521%, with respect to R21 and R22, the overall agreement in this case between simulated liquid temperature profile and measurements is generally good.

From the results of Table 2, regarding the Cases 3.a–3.e for all runs, it has been noticed that it leads to the same conclusions.

9.4 Vapor pressure

Different correlations for vapor pressure estimation (see Tab. A5) were employed to simulate the liquid temperature and the liquid CO_2 loading using the experimental data of Sonderby *et al.* (2013), the results for R21 and R22 are illustrated in Figure 3.

As shown in Figure 3, the influence of the vapor pressure on both, the liquid temperature and the liquid CO_2 loading is important. According to runs R21 and R22, the results obtained while using the correlation developed by Antoine (1888) show a good agreement with experimental data, contrary to the correlation suggested by Riedel (1954)

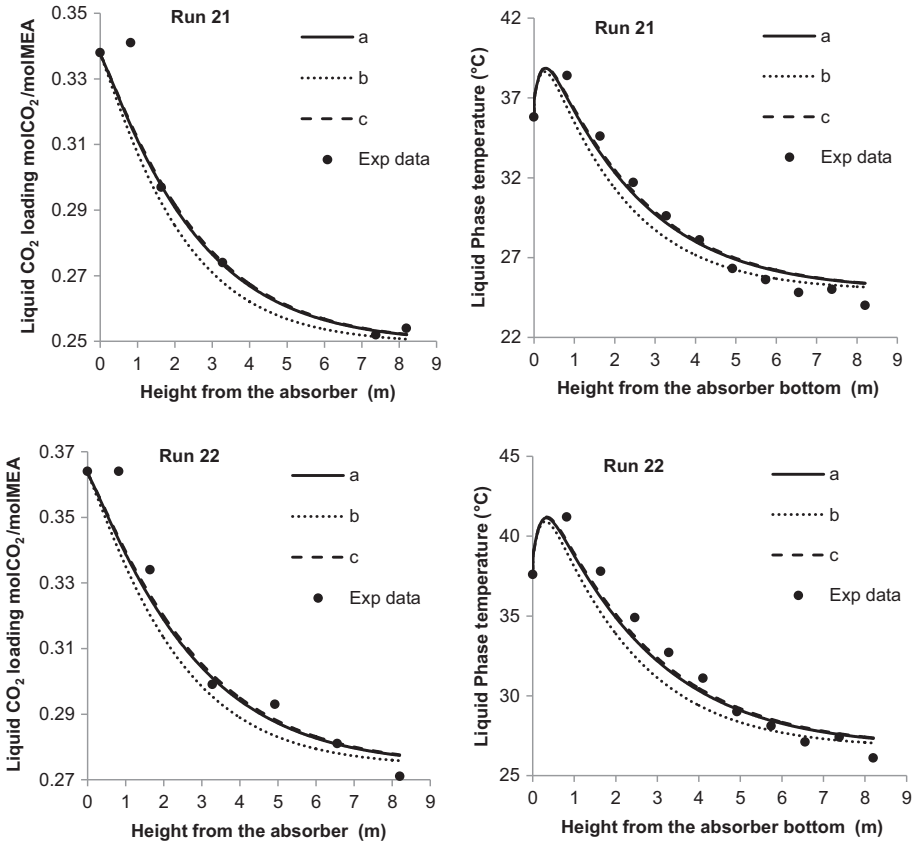

Fig. 4. Simulation results obtained using different cases of CO_2 diffusivity correlations in aqueous MEA solution: (a) Ko *et al.* (2001), (b) Jamal (2002) and (d) Ying and Eimer (2012).

where the ARD% is very large (see Tab. 2), it overestimates the liquid temperature and the liquid CO_2 loading, while the use of Ambrose and Walton (1989) correlation under-predicts them. All in all, and according to these results as well as the results shown in Table 2 for the Cases 4.a–4.d, it has been concluded that the correlation developed by Antoine (1888) leads to the most accurate simulation results.

9.5 CO_2 diffusivity in aqueous solutions of MEA

The influence of CO_2 diffusivity in aqueous solutions of MEA on the column performance is studied by using the measurements taken from Sonderby *et al.* (2013). The results, shown in Figure 4, are presented in terms of liquid temperature and liquid CO_2 loading.

According to this figure, It has been noticed that the influence of the CO_2 diffusivity in aqueous MEA solution on the column performance is not very large, all the three correlations show a good agreement with experimental data, the profiles obtained from the correlations of Ko *et al.* (2001) and Ying and Eimer (2012) are almost overlapped with very close ARD%s (see Tab. 2). However, the use of the correlation of Jamal (2002) under-predicts both, liquid temperature and liquid CO_2 loadings profiles. The lowest ARD% is obtained from the correlation suggested by Ying and Eimer (2012), while the highest ARD% is given from the correlation developed by Jamal (2002), and according to Table 2 for the cases 5.a–5.c, the same is observed for the other runs.

9.6 The added value of this study to the modeling and simulation

In general, the experimental techniques, the number of measurements, as well as the assumptions behind the different model parameter correlations are the main reason of the discrepancies between experimental data and simulated profiles, therefore, a good selection of such correlations is of high importance which is the key objective of this parametric study. And in order to prove its significance on obtaining reliable modeling and simulation results, a comparison between a combination of different model parameters that present the highest and the lowest ARDs% was performed (only this two cases were chosen since the number of possible combinations is very large), in other words, the difference in deviation between the worst case and the best one is investigated in this section, Table 3 summarized the model parameter correlations used in each case.

According to the comparison results illustrated in Figure 5, for different runs (R 3, 8, 13–15, 18, 21–23) of Sonderby *et al.* (2013), we can come up with the following conclusions:

Table 3. List of the different model parameter correlations used in each case.

Model properties	Case 1	Case 2
Kinetic model	Aboudheir *et al.* (2003)	Luo *et al.* (2015)
Enhancement factor	Cussler (2009)	Van Krevelen and Hoftijzer (1948)
Heat of absorption	Llano-Restrepo and Araujo-Lopez (2015) based on Kim and Svendsen (2007) data	Llano-Restrepo and Araujo-Lopez (2015) based on Arcis *et al.* (2011) data
Vapor pressure	Riedel (1954)	Antoine (1888)
CO_2 diffusivity	Jamal (2002)	Ying and Eimer (2012)

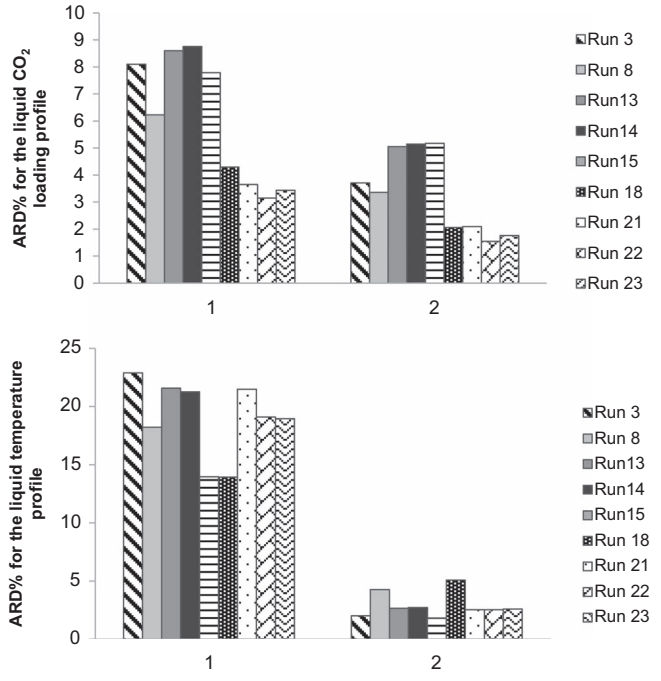

Fig. 5. Comparison results for runs (R 3, 8, 13–15, 18, 21–23) of Sonderby *et al.* (2013).

In general, the decrease of the model deviation between both cases is very large, it can reach more than 18% and 4% for the liquid temperature and liquid CO_2 loading profiles, respectively, which is more important for the liquid temperature than for the liquid CO_2 loading. This could be explained by the fact that almost all the model parameters studied in this paper have a great impact on the liquid temperature contrary to the liquid CO_2 loading where the influence is minor. Finally, this comparison shows clearly the significance of this study on obtaining reliable model predictions seen the important reduction of the model deviation obtained while estimating the model parameters by the means of the most accurate correlations.

10 Conclusion

One of the challenges faced while modeling and simulating the reactive absorption of CO_2 into loaded aqueous monoethanolamine solution in a packed-bed absorber is the proper calculation of the model parameters, hence, a parametric study was performed by using different cases of five different model parameters (kinetic model, enhancement factor, heat of absorption, CO_2 diffusivity in aqueous solutions of MEA, and vapor pressure). Consequently, the following points can be deduced:

- Among the model parameters studied in this paper, only kinetic model and vapor pressure have a large influence on the liquid CO_2 loading.
- Some parameters present a large influence on the liquid temperature (kinetic model, heat of absorption, and vapor pressure). Therefore, they should be chosen very carefully.
- The effect of the enhancement factor and CO_2 diffusivity is not very important, hence, a wrong choice of the model does not lead to severe deviation.
- The kinetic model introduced by Luo *et al.* (2015), the widely used model developed by Van Krevelen and Hoftijzer (1948) for the enhancement factor prediction, the developed correlation of Llano-Restrepo and Araujo-Lopez (2015) on the basis of Arcis *et al.* (2011) data for the heat of absorption estimation, vapor pressure expression of Antoine (1888), and the correlation of Ying and Eimer (2012) for the diffusivity of CO_2 in loaded aqueous MEA solution calculation generally provide more accurate predictions of the empirical values relative to the other cases employed in this analysis. This combination of correlations is obtained using the step-by step approach where the coupling between different processes or phenomena is neglected. Therefore, another optimum model could be found while using another methods of performing the paramedic study.

In addition, the comparison between the two combinations of different model parameters that present the highest and the lowest ARDs% revealed that the model deviation

could be reduced by 18% and 4% for the liquid temperature and liquid CO_2 loading profiles, respectively.

Funding sources

This research did not receive any specific grant from funding agencies in the public, commercial, or not-for-profit sectors.

References

Aboudheir A., Tontiwachwuthikul P., Chakma A., Idem R. (2003) Kinetics of the reactive absorption of carbon dioxide in high CO_2-loaded, concentrated aqueous monoethanolamine solutions, *Chem. Eng. Sci.* **58**, 5195–5210.

Abu-Zahra M.R.M., Shneiders L.H.J., Niederer J.P.M., Feron P.H.M., Versteeg G.F. (2007) CO_2 capture from power plants. Part I. A parametric study of the technical performance based on monoethanolamine, *Int. J. Greenh. Gas Control.* **1**, 37–46.

Afkhamipour M., Mofarahi M. (2013) Comparison of rate-based and equilibrium-stage models of a packed column for post-combustion CO_2 capture using 2-amino-2-methyl-1-propanol (AMP) solution, *Int. J. Greenh. Gas Control.* **15**, 186–199.

Afkhamipour M., Mofarahi M. (2014) Sensitivity analysis of the rate-based CO_2 absorber model using amine solutions (MEA, MDEA and AMP) in packed columns, *Int. J. Greenh. Gas Control.* **25**, 9–22.

Agbonghae E.O., Hughes K.J., Ingham D.B., Ma L., Pourkashanian M. (2014) A semi-empirical model for estimating the heat capacity of aqueous solutions of alkanolamines for CO_2 capture, *Ind. Eng. Chem. Res.* **53**, 8291–8301.

Akinola T.E., Oko E., Wang M. (2019) Study of CO_2 removal in natural gas process using mixture of ionic liquid and MEA through process simulation, *Fuel* **236**, 135–146.

Ali Saleh Bairq Z., Gao H., Huang Y., Zhang H., Liang Z. (2019) Enhancing CO_2 desorption performance in rich MEA solution by addition of $SO_4^{2-}/ZrO_2/SiO_2$ bifunctional catalyst, *Appl. Energ.* **252**, 113440.

Ambrose D., Walton J. (1989) Vapor pressures up to their critical temperatures of normal alkanes and 1-alkanols, *Pure Appl. Chem.* **61**, 1395–1403.

Antoine C. (1888) Tensions of the vapors, new relationship between the voltages and temperatures, *Rec. Meet. Acad. Sci.* **107**, 681–684.

Arcis H., Ballerat-Busserolles K., Rodier L., Coxam J.-Y. (2011) Enthalpy of solution of carbon dioxide in aqueous solutions of monoethanolamine at temperatures of 322.5 K and 372.9 K and pressures up to 5 MPa, *J. Chem. Eng. Data.* **56**, 3351–3362.

Billet R., Schultes M. (1999) Prediction of mass transfer columns with dumped and arranged packings, *Chem. Eng. Res. Des.* **77**, 498–504.

Blauwhoff P.M.M., Versteeg G.F., van Swaaij W.P.M. (1983) A study on the reaction between CO_2 and alkanolamines in aqueous solutions, *Chem. Eng. Sci.* **38**, 1411–1429.

Brian P.L.T., Hurley J.F., Hasseltine E.H. (1961) Penetration theory for gas absorption accompanied by a second order chemical reaction, *AIChE J.* **7**, 226–231.

Carson J.K., Marsh K.N., Mather A.E. (2000) Enthalpies of solution of carbon dioxide in (water + MEA or DEA or MDEA) and (water +MEA + MDEA) at 298.15 K, *J. Chem. Thermodyn.* **32**, 1285–1296.

Clarke J.K.A. (1964) Kinetics of absorption of carbon dioxide in monoethanolamine at short contact times, *Ind. Eng. Chem. Fundam.* **3**, 239–245.

Cullen E.J., Davidson J.F. (1957) Absorption of gas in liquid jet, *Trans. Faraday. Soc.* **53**, 113–120.

Cussler E.L. (2009) *Diffusion-mass transfer in fluid systems*, 3rd edn., Cambridge University Press, Cambridge.

Danckwerts P.V., Sharma M.M. (1966) The absorption of carbon dioxide into solutions of alkalis and amines, *Chem. Eng.* **10**, 244–280.

Dang H., Rochelle G.T. (2003) CO_2 Absorption Rate and Solubility in Monoethanolamine/Piperazine/Water, *Sep. Sci. Technol.* **38**, 337–357.

DeCoursey W.J. (1982) Enhancement factors for gas absorption with reversible reaction, *Chem. Eng. Sci.* **37**, 1483–1489.

DeCoursey W.J., Thring R.W. (1989) Effects of unequal diffusivities on enhancement factors for reversible and irreversible reaction, *Chem. Eng. Sci.* **44**, 1715–1721.

Dugas R.E., Rochelle G.T. (2011) CO_2 absorption rate into concentrated aqueous monoethanolamine and piperazine, *J. Chem. Eng. Data.* **56**, 2187–2195.

Faramarzi L. (2010) Post-combustion capture of CO_2 from fossil fuelled power plants, *PhD Thesis*, Department of Chemical and Bimolecular Engineering, Technical University of Denmark.

Freguia S., Rochelle G.T. (2003) Modeling of CO_2 capture by aqueous monoethanolamine, *Am. Inst. Chem. Eng. J.* **49**, 1676–1686.

Gaspar J., Fosbøl P.L. (2015) A general enhancement factor model for absorption and desorption systems: A CO_2 capture case-study, *Chem. Eng. Sci.* **138**, 203–215.

Geankoplis C.J. (2003) *Transport processes and separation process principles*, 4th edn., Prentice-Hall.

Gheni S.A., Abed M.F., Halabia E.K., Ahmed S.R. (2018) Investigation of carbon dioxide (CO_2) capture in a falling film contactor by computer simulation, *Oil Gas Sci. Technol. - Rev. IFP Energies nouvelles* **73**, 43.

Gilliland E.R., Baddour R.F., Brian P.L.T. (1958) Gas absorption accompanied by a liquid-phase chemical reaction, *AIChE J.* **4**, 223–230.

Hatta S. (1928) *Technical reports*, Tohoku Imperial University, Sendai.

Hikita H., Asai S., Ishikawa H., Honda M. (1977) The kinetics of reactions of carbon dioxide with monoethanolamine, diethanolamine and triethanolamine by a rapid mixing method, *Chem. Eng. J.* **13**, 7–12.

Hikita H., Asai S., Katsu Y., Ikuno S. (1979) Absorption of carbon dioxide into aqueous monoethanolamine solutions, *Am. Inst. Chem. Eng. J.* **25**, 793–800.

Hikita H., Asai S., Yano A., Nose H. (1982) Kinetics of absorption of carbon dioxide into aqueous sodium sulfite solutions, *AIChE J.* **28**, 1009–1015.

Hogendoorn J.A., Vas Bhat R.D., Kuipers J.A.M., Van Swaaij W.P.M., Versteeg G.F. (1997) Approximation for the enhancement factor applicable to reversible reactions of finite rate in chemically loaded solutions, *Chem. Eng. Sci.* **52**, 4547–4559.

Holderbaum T., Gmehling J. (1991) PSRK: a group contribution equation of state based on UNIFAC, *Fluid. Phase. Equilib.* **70**, 251–265.

Horng S.Y., Li M.H. (2002) Kinetics of absorption of carbon dioxide into aqueous solutions of monoethanolamine + triethanolamine, *Ind. Eng. Chem. Res.* **41**, 257–266.

IPCC (2007) *Intergovernmental panel on climate change fourth assessment report: Climate change 2007-mitigation of climate change*, Cambridge University Press, Cambridge.

Jamal A. (2002) Absorption and desorption of CO_2 and CO in alkanolamine systems, *PhD Thesis*, University of British Columbia, Canada.

Jamal A., Meisen A., Lim C.J. (2006) Kinetics of carbon dioxide absorption and desorption in aqueous alkanolamine solutions using a novel hemispherical contactor: experimental results and parameter estimation, *Chem. Eng. Sci.* **61**, 6590–6603.

Jayarathna S.A., Weerasooriya A., Dayarathna S., Eimer D.A., Melaaen M.C. (2013) Densities and surface tensions of CO_2 loaded aqueous monoethanolamine solutions with r = (0.2 to 0.7) at T = (303.15 to 333.15) K, *J. Chem. Eng. Data.* **58**, 986–992.

Jiru Y., Eimer D.A., Wenjuan Y. (2012) Measurements and correlation of physical solubility of carbon dioxide in (monoethanolamine + water) by a modified technique, *Ind. Eng. Chem. Res.* **51**, 6958–6966.

Kell G.S. (1975) Density, thermal expansivity, and compressibility of liquid water from 0 to 150 C: Correlations and tables for atmospheric pressure and saturation reviewed and expressed on 1968 temperature scale, *J. Chem. Eng. Data.* **20**, 97–105.

Khan F.M., Krishnamoorthi V., Mahmud T. (2011) Modeling reactive absorption of CO_2 in packed columns for post-combustion carbon capture applications, *Chem. Eng. Res. Des.* **89**, 1600–1608.

Kim I. (2009) Heat of Reaction and Vapor-Liquid Equilibrium of Post Combustion CO2 Absorbents, *PhD Thesis*, Norwegian University of Science and Technology, Trondheim, Norway.

Kim I., Svendsen H.F. (2007) Heat of absorption of carbon dioxide (CO_2) inmonoethanolamine (MEA) and 2-(aminoethyl) ethanolamine (AEEA) solutions, *Ind. Eng. Chem. Res.* **46**, 5803–5809.

Ko J.J., Tsai T.C., Lin C.Y. (2001) Diffusivity of nitrous oxide in aqueous alkanolamine solutions, *J. Chem. Eng. Data.* **46**, 160–165.

Kohl A.L., Nielsen R.B. (1997) *Gas purification*, 5th edn., Gulf Publishing Co, Houston.

Kucka L., Kenig E.Y., Górak A. (2002) Kinetics of the gas–liquid reaction between carbon dioxide and hydroxide ions, *Ind. Eng. Chem. Res.* **41**, 5952–5957.

Kucka L., Richter J., Kenig E.Y., Górak A. (2003) Determination of gas–liquid reaction kinetics with a stirred cell reactor, *Sep. Purif. Technol.* **31**, 163–175.

Kvamsdal H.M., Rochelle G. (2008) Effects of the temperature bulge in CO_2 absorption from flue gas by aqueous monoethanolamine, *Ind. Eng. Chem. Res.* **47**, 867–875.

Kvamsdal H.M., Jakobsen J.P., Hoff K.A. (2009) Dynamic modeling and simulation of a CO_2 absorber column for post-combustion CO_2 capture, *Chem. Eng. Process.* **48**, 135–144.

Kvamsdal H.M., Hillestad M. (2012) Selection of model parameter correlations in a rate-based CO_2 absorber model aimed for process simulation, *Int. J. Greenh. Gas Control.* **11**, 11–20.

Last W., Stichlmair J. (2002) Determination of mass transfer parameters by means of chemical absorption, *Chem. Eng. Technol.* **25**, 385–391.

Li M.H., Lai M.D. (1995) Solubility and Diffusivity of N_2O and CO_2 in (Monoethanolamine + N-Methyldiethanolamine + Water) and in (Monoethanolamine + 2-Amino-2-Methyl-1-Propanol + Water), *J. Chem. Eng. Data.* **40**, 486–492.

Littel R.J., Versteeg G.F., Van Swaaij W.P.M. (1992) Kinetics of CO_2 with primary and secondary amines in aqueous solutions-II. Influence of temperature on zwitterion formation and deprotonation rates, *Chem. Eng. Sci.* **47**, 2037–2045.

Liu F., Fang M., Dong W., Wang T., Xia Z., Wang Q., Luo Z. (2019) Carbon dioxide absorption in aqueous alkanolamine blends for biphasic solvents screening and evaluation, *Appl. Energy* **234**, 468–477.

Llano-Restrepo M., Araujo-Lopez E. (2015) Modeling and simulation of packed-bed absorbers for post-combustion capture of carbon dioxide by reactive absorption in aqueous monoethanolamine solutions, *Int. J. Greenh. Gas Control.* **42**, 258–287.

Luo X., Hartono A., Hussain S., Svendsen H.F. (2015) Mass transfer and kinetics of carbon dioxide absorption into loaded aqueous monoethanolamine solutions, *Chem Eng Sci.* **123**, 57–69.

Luo X., Hartono A., Svendsen H.F. (2012) Comparative kinetics of carbon dioxide absorption in unloaded aqueous monoethanolamine solutions using wetted wall and string of discs columns, *Chem. Eng. Sci.* **82**, 31–43.

Mathonat C., Majer V., Mather A.E., Grolier J.P.E. (1998) Use of solubility of CO_2 in aqueous monoethanolamine solutions, *Ind. Eng. Chem. Res.* **37**, 4136–4141.

Mehassouel A., Derriche R., Bouallou C. (2018) Kinetics study and simulation of CO_2 absorption into mixed aqueous solutions of methyldiethanolamine and hexylamine, *Oil Gas Sci. Technol. - Rev. IFP Energies nouvelles* **73**, 19.

Mofarahi M., Khojasteh Y., Khaledi H., Farahnak A. (2008) Design of CO_2 absorption plant for recovery of CO_2 from flue gases of gas turbine, *Energy* **33**, 1311–1319.

Mohammadpour A., Mirzaei M., Azimi A. (2019) Dimensionless numbers for solubility and mass transfer rate of CO_2 absorption in MEA in presence of additives, *Chem. Eng. Res. Des.* **151**, 207–213.

Pandya J.D. (1983) Adiabatic gas absorption and stripping with chemical reaction in packed towers, *Chem. Eng. Commun.* **19**, 343–361.

Pinsent B.R., Pearson L., Roughton F.J.W. (1956) The kinetics of combination of carbon dioxide with hydroxide ions, *Trans. Faraday Soc.* **52**, 1512–1520.

Pitzer K.S., Curl R.F. (1957) *The thermodynamic properties of fluids*, Institution of Mechanical Engineers, London.

Plaza J.M. (2011) Modeling of carbon dioxide absorption using aqueous monoethanolamine, piperazine and promoted potassium carbonate, *PhD Thesis*, The University of Texas at Austin, Austin, TX.

Poling B.E., Prausnitz J.M., O'Connell J.P. (2001) *The properties of gases and liquids*, McGraw-Hill, New York.

Puxty G., Rowland R., Attalla M. (2010) Comparison of the rate of CO_2 absorption into aqueous ammonia and monoethanolamine, *Chem. Eng. Sci.* **65**, 915–922.

Reid R.C., Prausntiz J.M., Poling B.E. (1987) *The Properties of Gases and Liquids*, Mc-Graw Hill, New York.

Riedel L. (1954) Extension of the theorem of corresponding states. III. Critical coefficient, density of saturated vapor, and latent heat of vaporization, *Chem. Ing. Tech.* **26**, 679–683.

Sada E., Kumazawa H., Butt M.A. (1978) Solubility and diffusivity of gases in aqueous solutions of amines, *J. Chem. Eng. Data* **23**, 161–163.

Smith J.M., van Ness H.C., Abbott M.M. (2005) *Introduction to chemical engineering thermodynamics*, 7th edn., McGraw-Hill, New York.

Snijder E.D., te Riele M.J.M., Versteeg G.F., Van Swaaij W.P.M. (1993) Diffusion coefficients of several aqueous alkanolamine solutions, *J. Chem. Eng. Data* **38**, 475–480.

Soave G. (1972) Equilibrium constants from a modified Redlich-Kwong equation of state, *Chem. Eng. Sci.* **27**, 1197–1203.

Sonderby T.L., Carlsen K.B., Fosbol P.L., Kiorboe L.G., Von Solms N. (2013) A new pilot absorber for CO_2 capture from flue gases: measuring and modeling capture with MEA solution, *Int. J. Greenh. Gas Control.* **12**, 181–192.

Treybal R.E. (1969) Adiabatic gas absorption and stripping in packed towers, *Ind. Eng. Chem.* **61**, 36–41.

Van Krevelen D.W., Hoftijzer P.J. (1948) Kinetics of gas–liquid reactions. Part I. General theory, *Recl. Trav. Chim. Pays-Bas.* **67**, 563–586.

Van Swaaij W.P.M., Versteeg G.F. (1992) Mass transfer accompanied with complex reversible chemical reactions in gas-liquid systems: an overview, *Chem. Eng. Sci.* **47**, 3181–3195.

Van Wijngaarden G.D.L., Versteeg G.F., Beenackers A.A.C.M. (1986) Mass-transfer enhancement factors for reversible gas-liquid reactions: comparison of DeCoursey's and Onda's methods, *Chem. Eng. Sci.* **41**, 2440–2442.

Versteeg G.F., Kuipers J.A.M., Van Beckum F.P.H., Van Swaaij W.P.M. (1989) Mass transfer with complex reversible chemical reactions-I. Single reversible chemical reaction, *Chem. Eng. Sci.* **44**, 2295–2310.

Versteeg G.F., van Dijck L.A.J., van Swaaij W.P.M. (1996) On the kinetics between CO_2 and alkanolamines both in aqueous and non-aqueous solutions: an overview, *Chem. Eng. Commun.* **144**, 113–158.

Wang J., Deng S., Sun T., Xu Y., Li K., Zhao J. (2019) Thermodynamic and cycle model for MEA-based chemical CO_2 absorption, *Energy Procedia.* **158**, 4941–4946.

Wang T., Yu W., Liu F., Fang M., Farooq M., Luo Z. (2016) Enhanced CO_2 absorption and desorption by MEA based nanoparticle suspensions, *Ind. Eng. Chem. Res.* **55**, 7830–7838.

Weast R.C. (1984) *Handbook of Chemistry and Physics*, 65th edn., CRC.

Weiland R.H., Dingman J.C., Cronin D.B., Browning G.J. (1998) Density and Viscosity of Some Partially Carbonated Aqueous Alkanolamine Solutions and Their Blends, *J. Chem. Eng. Data.* **43**, 378–382.

Wellek R.M., Brunson R.J., Law F.H. (1978) Enhancement factors for gas-absorption with second-order irreversible chemical reaction, *Can. J. Chem. Eng.* **56**, 181–186.

Wilke C.R. (1950) Diffusional properties of multicomponent gases, *Chem. Eng. Prog.* **46**, 95–104.

Wu Y., Zhou Q., Chan C.W. (2010) A comparison of two data analysis techniques and their applications for modeling the carbon dioxide capture process, *Eng. Appl. Artif. Intell.* **23**, 1265–1276.

Yeramian A.A., Gottifredi J.C., Ronco J.J. (1970) Mass transfer with homogeneous second order irreversible reaction a note on an explicit expression for the reaction factor, *Chem. Eng. Sci.* **25**, 1622–1625.

Ying J., Eimer D.A. (2012) Measurements and correlations of diffusivities of nitrous oxide and carbon dioxide in monoethanolamine + water by Laminar liquid jet, *Ind. Eng. Chem. Res.* **51**, 16517–16524.

Ying J., Eimer D.A. (2013) Determination and measurements of mass transfer kinetics of CO_2 in concentrated aqueous monoethanolamine solutions by a stirred cell, *Ind. Eng. Chem. Res.* **52**, 2548–2559.

Appendix

Table A1. List of correlations used for the calculation of physicochemical and transport properties.

Liquid phase properties			
Property	Correlation	Property	Correlation
Density of pure MEA	Jayarathna *et al.* (2013)	Henry's constant of N_2O in aqueous MEA solution	Jiru *et al.* (2012)
Density of water	Kell (1975)	Diffusivity of MEA in water	Snijder *et al.* (1993)
Density of CO_2-loaded MEA solution	Weiland *et al.* (1998)	Surface Tension of CO_2-loaded aqueous MEA solution	Jayarathna *et al.* (2013)
Viscosity of water	Swindells taken from Weast (1984)	Heat capacity of liquid MEA	Agbonghae *et al.* (2014)
Viscosity of CO_2-loaded MEA solution	Weiland *et al.* (1998)	Heat capacity of liquid water	Agbonghae *et al.* (2014)
Henry's constant of CO_2 in water	Jamal (2002)	Heat capacity of CO_2-loaded aqueous MEA solution	Agbonghae *et al.* (2014)
Henry's constant of N_2O in water	Jamal (2002)	Heat of vaporization	Pitzer and Curl (1957)
Gas phase properties			
Gas phase density	Soave (1972); Holderbaum and Gmehling (1991)	Gas phase CO_2 diffusivity	Wilke (1950)
Gas phase viscosity	Poling *et al.* (2001)	Thermal conductivity of pure gases	Ely and Hanley method taken from Reid *et al.* (1987)
Gas phase heat capacities	Smith *et al.* (2005)	Gas phase thermal conductivity	Wassiljewa-Mason-Saxen method taken from Poling *et al.* (2001)
Gas phase binary diffusivities	Fuller method taken from Poling *et al.* (2001)	Gas phase water vapor diffusivity	Blanc's expression taken from Poling *et al.* (2001)
Mass and heat transfer properties			
Mass transfer coefficients	Billet and Schultes (1999)	Gas phase heat transfer coefficient	Geankoplis (2003)
Effective interfacial area	Billet and Schultes (1999)	Mass-transfer-corrected gas-phase heat transfer coefficient	Pandya (1983)
Liquid holdup of packing	Billet and Schultes (1999)		

Table A2. Summary of kinetic models for CO_2 reacting with loaded aqueous MEA solution.

References	Mechanism type	Validity ranges	Kinetic constant expressions
Aboudheir *et al.* (2003)	Termolecular mechanism	3–9 M	$k_2 = \sum_i k_{2,i}[\text{base}, i]$
		293–333 K	$k_2 = k_{2,\text{MEA}}[\text{MEA}] + k_{2,\text{H}_2\text{O}}[\text{H}_2\text{O}]$
		0.1–0.5 mole CO_2/mole MEA	$k_{2,\text{MEA}} = 4.61 \times 10^9 \exp\left(\frac{-4412}{T_L}\right)$
			$k_{2,\text{H}_2\text{O}} = 4.55 \times 10^6 \exp\left(\frac{-3287}{T_L}\right)$
Luo *et al.* (2015)	Termolecular mechanism	1 and 5 M	$k_2 = \sum_i k_{2,i}[\text{base}, i]$
		298–343 K	$k_2 = k_{2,\text{MEA}}[\text{MEA}] + k_{2,\text{H}_2\text{O}}[\text{H}_2\text{O}]$
		0–0.4 mole CO_2/mole MEA	$k_{2,\text{MEA}} = 2.003 \times 10^{10} \exp\left(\frac{-4742}{T_L}\right)$
			$k_{2,\text{H}_2\text{O}} = 4.147 \times 10^6 \exp\left(\frac{-3110}{T_L}\right)$

Table A3. Summary of the enhancement factor models.

References	Reaction condition/Theory	Enhancement factor expressions
Van Krevelen and Hoftijzer (1948)	• 2nd order irreversible reaction	$\text{Ha} = \frac{\sqrt{k_2 C_\text{R} D_\text{A,L}}}{k^0_\text{L,A}}$
	• Film theory	$E_\text{i}^\text{film} = 1 + \left(\frac{C_\text{R} D_\text{R}}{\nu D_\text{A,L} C_\text{A,I}}\right)$
		$E^\text{film} = \frac{\text{Ha}\sqrt{\frac{E_i^\text{film} - E^\text{film}}{E_\text{i}^\text{film} - 1}}}{\tan h\left(\text{Ha}\sqrt{\frac{E_i^\text{film} - E^\text{film}}{E_i^\text{film} - 1}}\right)}$
Brian *et al.* (1961)	• Irreversible 2nd order reaction	$E_i^\text{pen} = \sqrt{\frac{D_\text{A,L}}{D_\text{R}}} + \sqrt{\frac{D_\text{R}}{D_\text{A,L}}}\left(\frac{C_\text{R}}{\nu C_\text{A,I}}\right)$
	• Penetration theory	$E^\text{pen} = \frac{\text{Ha}\sqrt{1 - \left(\frac{E_i^\text{pen} - 1}{E_i^\text{pen} - 1}\right)}}{\tan h\left(\text{Ha}\sqrt{1 - \left(\frac{E_i^\text{pen} - 1}{E_i^\text{pen} - 1}\right)}\right)}$
Yeramian *et al.* (1970)	• 2nd order irreversible reaction	$E_1^\text{pen} = \text{Ha}\left[\left\{1 + \frac{\pi}{8\text{Ha}^2}\right\}\text{erf}\left[\sqrt{\frac{4\text{Ha}^2}{\pi}}\right] + \frac{1}{2\text{Ha}} \exp\left(\frac{-4\text{Ha}^2}{\pi}\right)\right]$
	• Penetration and surface-renewal theories	$E_\text{i}^\text{pen} = 1 + \left(\frac{C_\text{R}}{\nu C_\text{A,I}}\right)$
		$E^\text{pen} = \frac{\left(E_1^\text{pen}\right)^2}{2\left(E_\text{i}^\text{pen} - 1\right)}\left[\sqrt{1 + \frac{4\left(E_\text{i}^\text{pen} - 1\right)E_\text{i}^\text{pen}}{\left(E_1^\text{pen}\right)^2}} - 1\right]$
		$E^\text{surf} = \frac{\text{Ha}^2}{2\left(E_\text{i}^\text{pen} - 1\right)}\left[\sqrt{1 + \frac{4\left[\left(E_\text{i}^\text{pen} - 1\right)^2 + E_\text{i}^\text{pen}\text{Ha}^2\left(E_\text{i}^\text{pen} - 1\right)\right]}{\text{Ha}^4}} - 1\right]$

(Continued on next page)

Table A3. (Continued)

References	Reaction condition/Theory	Enhancement factor expressions
Wellek *et al.* (1978)	• 2nd order irreversible reaction	$E_1^{\text{film}} = \frac{(\text{Ha})}{\tan h(\text{Ha})}$
	• Film theory	$E_{\text{i}}^{\text{film}} = 1 + \left(\frac{C_{\text{R}} D_{\text{R}}}{\nu D_{\text{A,L}} C_{\text{A,I}}}\right)$
		$E^{\text{film}} = 1 + \frac{1}{\left[(1/(E_{\text{i}}-1))^{1.35} + (1/E_1-1)^{1.35}\right]^{1/1.35}}$
Last and Stichlmair (2002)	• 2nd order irreversible reaction • Surface-renewal theory	$E^{\text{surf}} = 1 + \frac{1}{\left\{\left[1-1/\text{E}_{\text{i}}^{\text{film}}\right]/\text{Ha}^{3/2} + \left[1/\left(\text{E}_{\text{i}}^{\text{film}}\right)^{3/2}\right]\right\}^{2/3}}$
Cussler, 2009	• Fast reaction	$E^{\text{film}} = (\text{Ha})\ \cot h(\text{Ha})$
	• Film theory	
Gaspar and Fosbøl (2015)	• 2nd order reversible reaction	$E_{\text{i}}^{\text{film}} = 1 + \left(\frac{C_{\text{R}} D_{\text{R}}}{\nu D_{\text{A,L}} C_{\text{A,I}}}\right)$
	• Film theory	$\left(1 - E_{\text{i}}^{\text{film}}\right) Y^2 + \text{Ha}(y_{\text{A.I}} - 1)\, Y + E_{\text{i}}^{\text{film}} - y_{\text{A}} = 0$
		$Y = \sqrt{y_{\text{R}}^{\text{i}}}$
		$E^{\text{film}} = \text{Ha}\sqrt{y_{\text{R}}^{\text{i}}}\,\frac{1-y_{\text{A.I}}}{1-y_{\text{A}}}$

Table A4. Summary of heat of absorption correlations and fixed values.

References	Heat of absorption correlations and fixed values
Kohl and Nielsen (1997)	(118.2 kJ/mol)
Pandya (1983)	(84.4 kJ/mol)
Kim (2009)	$-\Delta H_{\text{rx}}^{(\text{abs})} = 84.68 - 0.1135 t_{\text{L}} + 0.0027 t_{\text{L}}^2$ $t_{\text{L}} = T_{\text{L}} - 273.15$
Llano-Restrepo and Araujo-Lopez (2015) based on Kim and Svendsen (2007) data	$-\Delta H_{\text{rx}}^{(\text{abs})} = 85.2903 - 38.5592\alpha_{\text{CO}_2} + 193.189(\alpha_{\text{CO}_2})^2 - 317.759(\alpha_{\text{CO}_2})^3 + 124.958(\alpha_{\text{CO}_2})^4$
Llano-Restrepo and Araujo-Lopez (2015) based on Arcis *et al.* (2011) data	$-\Delta H_{\text{rx}}^{(\text{abs})} = B_0 + B_1\alpha_{\text{CO}_2} + B_2(\alpha_{\text{CO}_2})^2 + B_3(\alpha_{\text{CO}_2})^3$ with: $B_0 = 111.171 - 4.62336\, P + 0.0772299 P^2$ $B_1 = -4..33417 + 12.6306\, P - 0.222593 P^2$ $B_2 = -72.9602 - 13.3031\, P + 0.244333 P^2$ $B_3 = 3.72612 + 7.62998\, P - 0.135737 P^2$

Table A5. Summary of water vapor-pressure correlations.

References	Correlations
Antoine (1888)	$P_S^{sat} = 10^5 \times 10^{\left[5.11564 - \frac{1687.537}{T_G + 230.17 - 273.15}\right]}$
Riedel (1954)	$P_S^{sat} = 10^5 \times \exp\left[\left(A^+ + \frac{B^+}{T_r} + C^+ \ln T_r + D^+ T_r^6\right) + \ln P_c\right]$ with:
	$A^+ = -35Q$
	$B^+ = -36Q$
	$C^+ = 42Q + \alpha_c$
	$D^+ = -Q$
	K *to be 0.0838*
	$Q = K(3.758 - \alpha_c)$
	$\alpha_c = \frac{3.758K\psi_b + ln(P_c/1.01325)}{K\psi_b - lnT_{br}}$
	$\psi_b = -35 + \frac{36}{T_{br}} + 42lnT_{br} - T_{br}^6$
Ambrose and Walton (1989)	$P_S^{sat} = 10^5 \times \exp\left[\left(f^{(0)} + \omega f^{(1)} + \omega^2 f^{(2)}\right) + \ln P_c\right]$
	$f^{(0)} = \frac{-5.97616(1-T_r) + 1.29874(1-T_r)^{1.5} - 0.60394(1-T_r)^{2.5} - 1.06841(1-T_r)^5}{T_r}$
	$f^{(1)} = \frac{-5.03365(1-T_r) + 1.11505(1-T_r)^{1.5} - 5.41217(1-T_r)^{2.5} - 7.46628(1-T_r)^5}{T_r}$
	$f^{(2)} = \frac{-0.64771(1-T_r) + 2.41539(1-T_r)^{1.5} - 4.26979(1-T_r)^{2.5} + 3.25259(1-T_r)^5}{T_r}$

Table A6. A list of CO_2 diffusivity correlations in aqueous MEA solution.

References	CO_2 diffusivity correlations
Ko *et al.* (2001)	$D^{\circ}_{N_2O} = 5.07 \times 10^{-6} \exp\left(\frac{-2371}{T_L}\right)$
	$D^{\circ}_{CO_2} = 2.35 \times 10^{-6} \exp\left(\frac{-2119}{T_L}\right)$
	$D_{N_2O,L} = \left(5.07 \times 10^{-6} + 8.65 \times 10^{-7} C_{MEA} + 2.78 \times 10^{-7} C^2_{MEA}\right) \times \exp\left[\frac{-2371 - 9.34 \times 10^1 C_{MEA}}{T_L}\right]$
	$D_{CO_2,L} = D_{N_2O,L}\left(\frac{D^{\circ}_{CO_2}}{D^{\circ}_{N_2O}}\right)$
Jamal (2002)	$D^{\circ}_{N_2O} = 5.2457 \times 10^{-6} \exp\left(\frac{-2388.9}{T_L}\right)$
	$D^{\circ}_{CO_2} = 3.7191 \times 10^{-6} \exp\left(\frac{-2257.9}{T_L}\right)$
	$D_{N_2O,L} = \left(5.2457 \times 10^{-6} + A_1 \times w_{MEA} + A_2 w^2_{MEA}\right) \times \exp\left[\frac{(-2388.9}{T_L}\right]$
	$A_1 = 1.4196 \times 10^{-5} - \frac{4.4209 \times 10^{-3}}{T_L}$
	$A_2 = -3.2060 \times 10^{-6} - \frac{9.8151 \times 10^{-4}}{T_L}$
	$D_{CO_2,L} = D_{N_2O,L}\left(\frac{D^{\circ}_{CO_2}}{D^{\circ}_{N_2O}}\right)$
Ying and Eimer (2012)	$D^{\circ}_{N_2O} = 5.07 \times 10^{-6} \exp\left(\frac{-2371}{T_L}\right)$
	$D^{\circ}_{CO_2} = 2.35 \times 10^{-6} \exp\left(\frac{-2119}{T_L}\right)$
	$D_{N_2O,L} = \left(5.07 \times 10^{-6} - 3.5443 \times 10^{-7} C_{MEA} + 3.4294 \times 10^{-9} C^2_{MEA}\right) \times \exp\left[\frac{(-2371 + 0.3749 \times C_{MEA}}{T_L}\right]$
	$D_{CO_2,L} = D_{N_2O,L}\left(\frac{D^{\circ}_{CO_2}}{D^{\circ}_{N_2O}}\right)$